Global synchronization of drive–response dynamical networks subject to input nonlinearity

2008 J. Phys. A: Math. Theor. 41 385103

(http://iopscience.iop.org/1751-8121/41/38/385103)

IOP Publishing — Journal of Physics A: Mathematical and Theoretical

J. Phys. A: Math. Theor. **41** (2008) 385103 (12pp) doi:10.1088/1751-8113/41/38/385103

Global synchronization of drive–response dynamical networks subject to input nonlinearity

Rong Li[1], **Zhisheng Duan**[1] **and Guanrong Chen**[2]

[1] State Key Laboratory for Turbulence and Complex Systems, Department of Mechanics and Aerospace Engineering, College of Engineering, Peking University, Beijing 100871, People's Republic of China

[2] Department of Electronic Engineering, City University of Hong Kong, Hong Kong SAR, People's Republic of China

E-mail: lirong@pku.edu.cn

Received 30 April 2008, in final form 24 July 2008
Published 22 August 2008
Online at stacks.iop.org/JPhysA/41/385103

Abstract

This paper investigates the global synchronization problem of complex dynamical networks consisting of a drive network and a response network. Using the decentralized and variable structure control techniques, a control law is derived which guarantees the global exponential synchronization of the drive–response network even with the presence of input nonlinearity. The proposed controller is applicable to complex networks with general nonlinear dynamical nodes. Chaotic networks are used as illustrative examples to demonstrate the effectiveness of the proposed control scheme.

PACS numbers: 89.75.−k, 05.45.Xt, 05.45.−a

(Some figures in this article are in colour only in the electronic version)

1. Introduction

Over the past few decades, the synchronization and control problems of complex dynamical networks have attracted a great deal of attention from the nonlinear dynamics community [1–16]. In the literature, the master stability function (MSF) approach [11], investigating the local stability of the synchronization manifold, has been extensively applied to the synchronization analysis and the synchronizability problem of complex dynamical networks [7–13]. And, based on the MSF approach, a control technique called pinning control has been successfully used to achieve network synchronization [17–21]. It should be noted that, because of the use of the local linearization method, the results obtained by the MSF approach are local.

So far, the studies of network synchronization have mostly been limited to within one network. Thus, a natural and interesting question is: does the synchronization happen between two coupled networks? Another question is what control scheme can be applied to this kind of synchronization problem. These questions deserve investigation for the ubiquitous existence of the collective dynamics between different complex communities, for example, the interplay between the prey and predator communities. In [22], the problem of synchronization between two coupled networks was also addressed by the approach of local stability analysis. In this paper, the problem of global synchronization of two coupled networks will be investigated.

Composed of many interconnected nodes, a general complex dynamical network can be seen as a high-dimensional nonlinear system. Therefore, implementing a centralized control scheme to such a system is difficult and expensive. In this paper, a decentralized control strategy, which is quite popular in large-scale systems theory [23–25], is used to achieve global synchronization of two coupled dynamical networks. Comparing with the centralized control strategy, decentralized control has many advantages for its lower dimensionality and using only individual node's information.

On the other hand, the control inputs of practical systems are usually subject to nonlinearity as a result of physical limitations. It has been shown that the input nonlinearity can cause a serious degradation of system performance, a reduced rate of response and in a worst-case scenario even system failure if the controller is not well designed [26]. Therefore, the effects of input nonlinearity should be taken into account when analyzing and implementing a control scheme, particularly for complex dynamical networks. Yet, a review of the existing literature reveals that the problem of controlling and synchronizing complex networks subject to input nonlinearity has not been carefully studied before.

In this paper, we will focus on the synchronization problem of two coupled networks with the drive–response (or unidirectional) coupling, in which one network does not receive any information from the other [27]. A variable structure control strategy, which is an effective method to synchronize two chaotic systems [28–32], is proposed to realize the global exponential synchronization of the drive–response networks subject to input nonlinearity. It is assumed, in this paper, that the nonlinear part of each individual node in the network is bounded and satisfies the Lipschitz condition. Obviously, many chaotic systems and Lur'e systems satisfy these conditions. And throughout this paper, for $x \in R^n$, the notation $\|x\| = (x^T x)^{\frac{1}{2}}$ denotes the Euclidean norm of vector x.

The remainder of the paper is organized as follows. In section 2, the synchronization problem of the drive–response network with the existence of input nonlinearity is formulated. In section 3, a proportional–integral (PI) switching surface, which means that the switching function is composed of the proportional and integral terms, is first formulated to simplify the task of determining the performance of the closed-loop error system in sliding motion. Then, a decentralized controller is designed, which is robust to the input nonlinearity and guarantees the global synchronization of the drive–response network. In section 4, numerical simulations are presented to demonstrate the effectiveness of the proposed controlled synchronization scheme. The paper is concluded by section 5.

2. Problem formulation

For two unidirectionally coupled complex dynamical networks, the network which does not receive any information from the other is called the drive network, while the other one is called the response network. Then, the drive network can be described as

$$\dot{x}_i(t) = Ax_i(t) + f(x_i(t)) + \theta \sum_{k=1}^{N} d_{ik}\Gamma x_k(t), \qquad i = 1, 2, \dots, N, \tag{1}$$

where $x_i(t) = [x_{i1}(t), x_{i2}(t), \ldots, x_{in}(t)]^T \in R^n$ is the n-dimensional state vector of node i, $A \in R^{n\times n}$ and $f(x_i(t)) = [f^1(x_i(t)), \ldots, f^n(x_i(t))]^T$ represent the linear part which can be zero and nonlinear part of the system dynamics of each individual node, respectively, constant $\theta > 0$ is the coupling strength, $\Gamma \in R^{n\times n}$ is the inner linking matrix, $D = (d_{ik}) \in R^{N\times N}$ is the coupling matrix representing the coupling configuration of the network. It is assumed that D is irreducible, with zero row-sum and not necessary to be symmetric.

Considering the unidirectional coupling and the input nonlinearity, the response network can be given by

$$\dot{z}_i(t) = Az_i(t) + f(z_i(t)) + \theta \sum_{k=1}^{N} d_{ik}\Gamma z_k(t) + \Phi_i(u_i(t)), \qquad i = 1, 2, \ldots, N, \tag{2}$$

where $z_i(t) \in R^n$ is the state vector of node i of the response network, A, $f(\cdot)$, θ, Γ and D are the same as given in (1). The term

$$\Phi_i(u_i(t)) = [\varphi_i(u_{i1}(t)), \ldots, \varphi_i(u_{in}(t))]^T, \qquad i = 1, 2, \ldots, N,$$

represents the nonlinear input of node i. Here, $u_i(t) = [u_{i1}(t), \ldots, u_{in}(t)]^T$ represents the controller needed to be designed for node i, where $u_{ij}(t)$, $j = 1, \ldots, n$, is the control item to be added to the jth function of node i; $\varphi_i : R \to R$ denotes some given nonlinear constraint on each u_{ij}. It is also assumed that φ_i is a continuous nonlinear function satisfying $\varphi_i(0) = 0$ and the following sector conditions:

$$\mu_{i,1}u_{ij}^2(t) \leqslant u_{ij}(t)\varphi_i(u_{ij}(t)) \leqslant \mu_{i,2}u_{ij}^2(t), \qquad j = 1, 2, \ldots, n, \tag{3}$$

where $\mu_{i,1}$ and $\mu_{i,2}$, $i = 1, 2, \ldots, N$, are nonzero positive constants.

Moreover, the following assumption is made regarding the nonlinear function f:

(H) $f : R^n \to R^n$ is bounded and satisfies the Lipschitz condition with a Lipschitz constant

$$L_i > 0, \text{ i.e. } \|f(x_i) - f(y_i)\| \leqslant L_i\|x_i - y_i\|, \qquad \text{for all} \quad x_i, y_i \in R^n, \quad i = 1, 2, \ldots, N.$$

The drive–response dynamical network as defined in (1) and (2) is said to achieve (asymptotical) synchronization if

$$e_i(t) = x_i(t) - z_i(t) \to 0, \qquad \text{as} \quad t \to \infty.$$

Note that the synchronization error equations of the drive–response network can be written as

$$\dot{e}_i(t) = Ae_i(t) + (f(e_i(t) + z_i(t)) - f(z_i(t))) + \theta \sum_{k=1}^{N} d_{ik}\Gamma e_k(t) - \Phi_i(u_i(t)),$$
$$i = 1, 2, \ldots, N. \tag{4}$$

Then, the objective is to design controllers $u_i \in R^{n\times 1}$, robust to the input nonlinearity φ_i, such that the synchronization error vector $e_i(t)$ satisfies $\lim_{t\to\infty}\|e_i(t)\| = 0$ even with different initial conditions $x_i(0)$ and $z_i(0)$, $i = 1, \ldots, N$.

3. Sliding mode controller design

From the variable structure control approach, to synchronize a drive–response dynamical network with nonlinear inputs involves two basic steps: (1) selecting an appropriate switching surface such that the sliding motion on the sliding manifold is stable and $\lim_{t\to\infty}\|e_i(t)\| = 0$; (2) establishing a robust control law which guarantees the existence of the sliding manifold $s_i(t) = 0$ even in the presence of the input nonlinearity.

Design the PI switching function $s_i(t)$ as

$$s_i(t) = \sigma_i e_i(t) - \int_0^t \sigma_i (A + K) e_i(\tau)\,\mathrm{d}\tau, \qquad i = 1, 2, \ldots, N, \tag{5}$$

where $s_i(t) \in R$, $K \in R^{n\times n}$ and $\sigma_i \in R^{1\times n}$, with $\sigma_{ik} \geqslant 0$ designable, $i = 1, \ldots, N, k = 1, \ldots, n$. Then, the equivalent control can be obtained from $\dot{s}_i(t) = 0$, which is a necessary condition for the state trajectory to stay on the switching surface $s_i(t) = 0$. Therefore, when the error system (4) operates in the sliding mode, the following differentiating equations need to be satisfied [33]:

$$\dot{s}_i(t) = \sigma_i(-K e_i(t) + (f(e_i(t) + z_i(t)) - f(z_i(t))) + \theta \sum_{k=1}^{N} d_{ik} \Gamma e_k(t) - \Phi_i(u_i(t))) = 0,$$
$$i = 1, 2, \ldots, N.$$

Solving the above equations, one obtains the equivalent control $\Phi_{i\mathrm{eq}}(u_i(t))$ as

$$\Phi_{i\mathrm{eq}}(u_i(t)) = -K e_i(t) + (f(e_i(t) + z_i(t)) - f(z_i(t))) + \theta \sum_{k=1}^{N} d_{ik} \Gamma e_k(t). \tag{6}$$

Substituting $\Phi_{i\mathrm{eq}}(u_i(t))$ into (4) shows that the error equations on the sliding surface are determined by

$$\dot{e}_i(t) = (A + K) e_i(t), \qquad i = 1, 2, \ldots, N. \tag{7}$$

Obviously, a feedback gain matrix K can be selected such that all eigenvalues of $A + K$ have negative real parts in order to guarantee the stability of (7). More significantly, the eigenvalues of $A + K$ are related to the exponential convergence speed of the error system in the sliding mode.

Note that the equivalent control $\Phi_{i\mathrm{eq}}(u_i(t))$ given in (6) is only a mathematically derived expression for the analysis of a sliding motion, but not a real control law being generated in practical systems. The equivalent control generates an ideal sliding motion on the switching surface, while a simple real variable structure controller to be designed will generate a trajectory close to the ideal sliding motion around the switching surface.

In what follows, a practical sliding mode control scheme is designed to drive the error system trajectories onto the sliding surface. The proposed control law $u_{ij}(t)$ is as follows:

$$u_{ij}(t) = \gamma_i (G_i \|e_i(t)\| + F_i) \frac{s_i(t)}{|s_i(t)| + \delta}, \qquad \gamma_i > \frac{1}{\mu_{i,1} \cdot \left(\sum_{k=1}^{n} \sigma_{ik}\right)},$$
$$i = 1, 2, \ldots, N, \quad j = 1, 2, \ldots, n, \tag{8}$$

where $G_i = (\|\sigma_i K\| + L_i \|\sigma_i\|)$, $F_i = \sum_{k=1}^{N} \theta \cdot |d_{ik}| \cdot \|\sigma_i \Gamma\| \cdot \|e_k(t)\|$, $\mu_{i,1}$ are given by (3), and δ is a sufficiently small designable constant used to eliminate possible chattering.

Theorem 1. *For the drive–response complex network given in (1) and (2), where function $f(\cdot)$ satisfies assumption (H), if the control input $u_{ij}(t)$ is defined by (8), then the trajectory of the error equation (4) converges to the sliding manifold $s_i(t) = 0$, $i = 1, 2, \ldots, N$.*

Proof. Take a Lyapunov function $V(t) = \sum_{i=1}^{N} |s_i(t)|$. Its time derivative is given by

$$\begin{aligned}\dot{V}(t) &= \sum_{i=1}^{N} \frac{s_i(t)\dot{s}_i(t)}{|s_i(t)|} \\ &= \sum_{i=1}^{N} \frac{s_i(t)}{|s_i(t)|} \cdot [\sigma_i(-Ke_i(t) + (f(e_i(t) + z_i(t)) - f(z_i(t))) \\ &\quad + \theta \sum_{k=1}^{N} d_{ik}\Gamma e_k(t) - \Phi_i(u_i(t)))].\end{aligned} \tag{9}$$

The first three terms on the right-hand side of (9) satisfy the following three inequalities, respectively:

$$\sum_{i=1}^{N} \frac{-s_i(t)\sigma_i K e_i(t)}{|s_i(t)|} \leqslant \sum_{i=1}^{N} \|\sigma_i K\| \cdot \|e_i(t)\|, \tag{10}$$

$$\begin{aligned}\sum_{i=1}^{N} \frac{s_i(t)\sigma_i(f(e_i(t) + z_i(t)) - f(z_i(t)))}{|s_i(t)|} &\leqslant \sum_{i=1}^{N} |\sigma_i(f(e_i(t) + z_i(t)) - f(z_i(t)))| \\ &\leqslant \sum_{i=1}^{N} L_i\|\sigma_i\| \cdot \|e_i(t)\|\end{aligned} \tag{11}$$

and

$$\sum_{i=1}^{N} \frac{s_i(t)\sigma_i\theta \sum_{k=1}^{N} d_{ik}\Gamma e_k(t)}{|s_i(t)|} \leqslant \sum_{i=1}^{N} \left|\sigma_i\theta \sum_{k=1}^{N} d_{ik}\Gamma e_k(t)\right| \leqslant \sum_{i=1}^{N}\sum_{k=1}^{N} \theta|d_{ik}| \cdot \|\sigma_i\Gamma\| \cdot \|e_k(t)\|. \tag{12}$$

Consider the last term on the right-hand side of (9). It follows from (3) and (8) that

$$\begin{aligned}u_{ij}(t)\varphi_i(u_{ij}(t)) &= \gamma_i(G_i\|e_i(t)\| + F_i)\frac{s_i(t)\varphi_i(u_{ij}(t))}{|s_i(t)| + \delta} \\ &\geqslant \mu_{i,1}(\gamma_i(G_i\|e_i(t)\| + F_i))^2 \frac{s_i^2(t)}{(|s_i(t)| + \delta)^2}.\end{aligned} \tag{13}$$

By (13), one has

$$s_i(t)\varphi_i(u_{ij}(t)) \geqslant \mu_{i,1}\gamma_i(G_i\|e_i(t)\| + F_i)\frac{s_i^2(t)}{(|s_i(t)| + \delta)}. \tag{14}$$

Furthermore, multiplying σ_{ij} on both sides of inequality (14) and summing up upon index j from 1 to n, one obtains

$$-\sum_{i=1}^{N} \frac{s_i(t)\sigma_i\Phi_i(u_i(t))}{|s_i(t)|} \leqslant -\sum_{i=1}^{N}\sum_{k=1}^{n} \sigma_{ik}\mu_{i,1}\gamma_i(G_i\|e_i(t)\| + F_i)\frac{s_i^2(t)}{|s_i(t)|(|s_i(t)| + \delta)}. \tag{15}$$

Substituting (10)–(12) and (15) into (9), one has

$$\begin{aligned}\dot{V}(t) &\leqslant \sum_{i=1}^{N}(G_i\|e_i(t)\| + F_i) - \sum_{i=1}^{N}\sum_{k=1}^{n} \sigma_{ik}\mu_{i,1}\gamma_i(G_i\|e_i(t)\| + F_i)\frac{|s_i(t)|}{(|s_i(t)| + \delta)} \\ &\leqslant \sum_{i=1}^{N}\left(1 - \mu_{i,1}\gamma_i\frac{|s_i(t)|}{(|s_i(t)| + \delta)}\sum_{k=1}^{n}\sigma_{ik}\right)(G_i\|e_i(t)\| + F_i).\end{aligned} \tag{16}$$

Since $\left(1 - \mu_{i,1}\gamma_i \sum_{k=1}^{n} \sigma_{ik}\right) < 0$ and δ is a designable parameter which can be chosen sufficiently small, inequality (16) implies $\dot{V}(t) < 0$. Therefore, $V(t)$ converges to zero, i.e. $s_i(t) \to 0, i = 1, 2, \ldots, N$. This completes the proof of the theorem. □

Theorem 2. *The error equation (4), in which function $f(\cdot)$ satisfies assumption (H), is asymptotically stable about zero if the control input $u_{ij}(t)$ is defined by (8).*

Proof. When the error equation (4) is driven by the control input $u_{ij}(t)$ given in (8), the trajectory of the error equation converges to the sliding manifold $s_i(t) = 0, i = 1, 2, \ldots, N$, by theorem 1. Thus, the equivalent control function $\Phi_{i\text{eq}}(u_i(t))$ in the sliding manifold can be obtained, as shown in (6). Substituting $\Phi_{i\text{eq}}(u_i(t))$ into (4), the equivalent error equation in the sliding manifold is obtained as shown in (7). As discussed above, the values of K are specified such that $(A+K)$ is stable in order to guarantee the asymptotical stability of (7). Consequently, the asymptotical stability of the error equation in (4) is ensured. The theorem is thus proved. □

Remark 1. In the proof of the stability of the error system (4), no linearizing technique is performed. Thus the above proposed control scheme theoretically guarantees the global synchronization of the drive–response network.

Remark 2. Note that there is no demand for the coupling matrix D to be symmetric in theorems of this section. Thus the proposed control scheme is applicable to the cases of weighted or oriented networks.

4. Numerical simulation

In order to show the effectiveness of the controller designed in section 3, numerical simulations are performed in this section by using the fourth-order Runge–Kutta method with time step size $t = 0.0025$.

Take Chua's oscillator as the individual node of the drive–response network. In the dimensionless form, Chua's oscillator is described by [34]

$$\begin{cases} \dot{x}_1 = \alpha(-x_1 + x_2 - g(x_1)), \\ \dot{x}_2 = x_1 - x_2 + x_3, \\ \dot{x}_3 = -\beta x_2 - \omega x_3, \end{cases} \tag{17}$$

where $g(\cdot)$ is a piecewise linear function:

$$g(x_1) = m_1 x_1 + \tfrac{1}{2}(m_2 - m_1)(|x_1 + 1| - |x_1 - 1|).$$

Take parameters $\alpha = 9, \beta = 14, \omega = 0.01, m_1 = -0.714$ and $m_2 = -1.14$, so that Chua's oscillator (17) generates a double-scroll chaotic attractor.

Suppose that both the drive and response networks are regular networks consisting of five Chua's oscillators. The drive network is described by

$$\dot{x}_i(t) = Ax_i(t) + f(x_i(t)) + \theta \sum_{k=1}^{5} d_{ik}\Gamma x_k(t), \qquad i = 1, 2, \ldots, 5, \tag{18}$$

where

$$x_i(t) = \begin{bmatrix} x_{i1}(t) \\ x_{i2}(t) \\ x_{i3}(t) \end{bmatrix}, \qquad A = \begin{bmatrix} -\alpha - \alpha m_1 & \alpha & 0 \\ 1 & -1 & 1 \\ 0 & -\beta & -\omega \end{bmatrix}, \qquad f(x_i) = \begin{bmatrix} f(x_{i1}) \\ 0 \\ 0 \end{bmatrix},$$

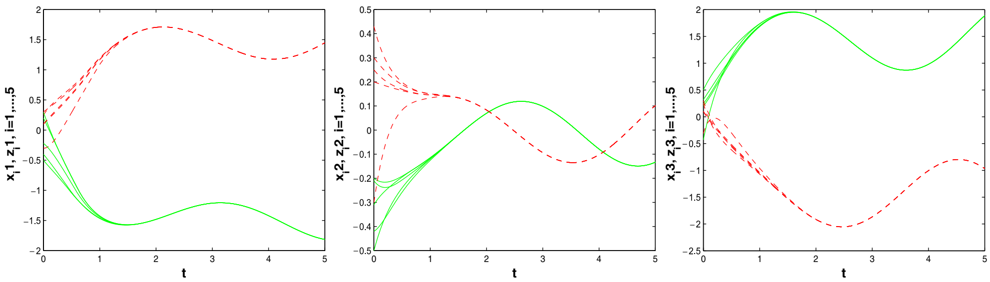

(*a*) (*b*) (*c*)

Figure 1. Evolutions of the state variables of two uncoupled networks with the same global coupling configuration and coupling strength.

$\Gamma = \mathrm{diag}\{1, 1, 1\}$ and $f(x_{i1}) = -\frac{1}{2}\alpha(m_2 - m_1)(|x_{i1} + 1| - |x_{i1} - 1|)$. Accordingly, the response network can be described as

$$\dot{z}_i(t) = Az_i(t) + f(z_i(t)) + \theta \sum_{k=1}^{5} d_{ik}\Gamma z_k(t) + \Phi_i(u_i(t)), \qquad i = 1, 2, \ldots, 5, \tag{19}$$

where $\Phi_i(u_i(t)) = [\varphi_i(u_{i1}(t)), \varphi_i(u_{i2}(t)), \varphi_i(u_{i3}(t))]^T$.

If $\Phi_i(u_i(t)) = 0$ in (19), i.e., without the control input, then because of the sensitive dependence on the initial conditions of chaotic systems, networks (18) and (19) will not synchronize in general. This phenomenon is shown in figure 1, where the green solid curves and the red dashed ones represent the trajectories of networks (18) and (19), respectively. The initial conditions of these two networks are random but different.

It can be verified that all the conditions required by theorems of section 3 are satisfied. Therefore, to achieve global synchronization, a control law as proposed in section 3 can be designed. Set $\varphi_i(u_{ij}(t))$, $j = 1, 2, 3$, be the same for node i, and denote by u_i the control input to node i. Suppose that the input nonlinearity is a periodic excitation modulated to the control input: $\varphi_i(u_{ij}(t)) = u_{ij}(t)[0.2\sin(u_{ij}(t)) + 0.9]$. Then, parameters $\mu_{i,1}$ and $\mu_{i,2}$ of (3) can be chosen as $\mu_{i,1} = 0.7$ and $\mu_{i,2} = 1.1$. It can be seen from the form of $f(x_{i1})$ that assumption (H) is satisfied with $L_i = 4$. Choose $\sigma_i = [2, 0, 0]$ and $\gamma_i = 0.75 > \frac{1}{\mu_{i,1}(\sum_{k=1}^{n}\sigma_{ik})}$. Assign the eigenvalues of $(A + K)$ to be $(-1, -2, -3)$, so a suitable K is determined as

$$K = \begin{bmatrix} 1.574 & -9 & 0 \\ -1 & -1 & -1 \\ 0 & 14 & -2.99 \end{bmatrix}.$$

Let the switching function $s_i(t)$ be in the form of (5) and choose $\delta = 0.1$. Then, the control law $u_{ij}(t)$ is designed according to (8), as follows:

$$u_{ij}(t) = 0.75\left[G_i\|e_i(t)\| + \sum_{k=1}^{N} 2\theta|d_{ik}| \cdot \|e_k(t)\|\right]\frac{s_i(t)}{|s_i(t)| + \delta}, \qquad i = 1, \ldots, 5,$$
$$j = 1, \ldots, 3. \tag{20}$$

Figure 2 shows the simulation results of the drive–response network with the global coupling configurations. The evolutions of state variables x_i and z_i are shown in figures 2(*a*)–(*c*) with the green solid curves and the red dashed ones denoting the trajectories of the drive network (18) and the response network (19), respectively. The evolutions of the corresponding error

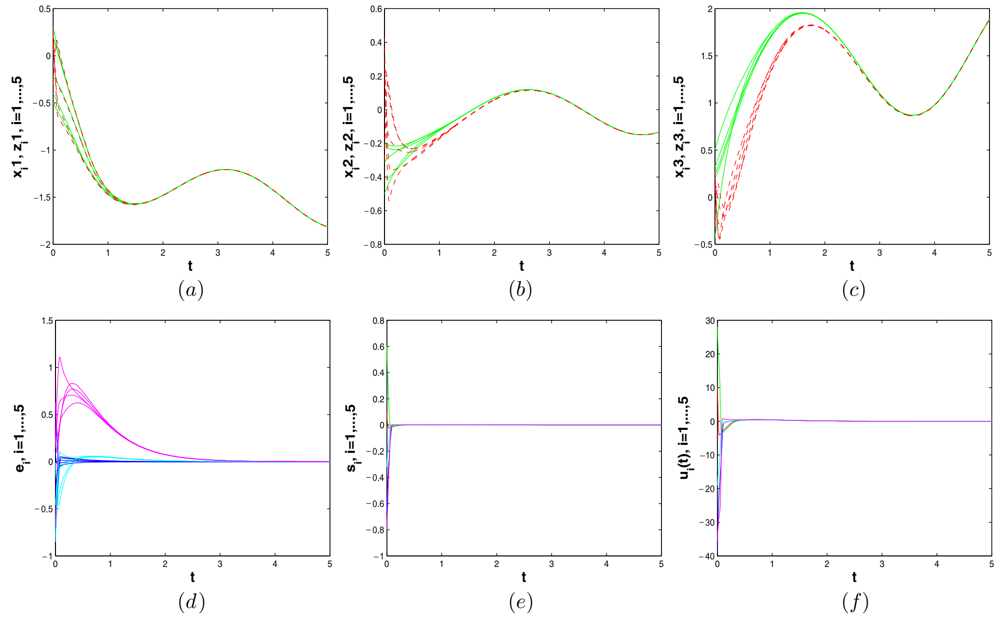

Figure 2. Synchronization of the drive–response network with the global coupling configuration and coupling strength $\theta = 1.5$. (a)–(c) Evolution of state variables x_i and z_i, (d) synchronization error states e_i, (e) time responses of s_i and (f) time responses of control inputs.

states are shown in figure 2(d). Figure 2(e) illustrates the time responses of s_i under the proposed control (20). Figure 2(f) shows the control inputs $u_i, i = 1, 2, \ldots, 5$.

From figure 2(c), one can clearly see that the synchronization of the drive–response network is slower than the internal synchronization of their own, respectively.

Remark 3. The initial conditions of networks (18) and (19) in figure 2 are the same as those in figure 1, where the differences of initial conditions of networks (18) and (19) are small. When the differences of these initial conditions are large, the drive–response network can still achieve synchronization under condition (20) through appropriate adjustment of parameters δ and time step size t. This is theoretically guaranteed by the global nature of the proposed control scheme. The simulations are similar as given in figure 2 and thus omitted.

Similarly, figure 3 shows the synchronization of the drive–response network with the star-shaped configuration. Both the drive network and the response network consist of five nodes; the color curve denotation and parameters are the same as those given above.

It can be seen from figure 3 that the synchronization of the star-shaped coupling network is slower than that of the global coupling network (see figure 2) when the same coupling strength is used.

Note that, the synchronization of the drive–response network does not depend on the internal synchronization of the drive network itself. Figure 4 shows the simulation results of the drive–response network (each with five nodes) with the global coupling configuration and coupling strength $\theta = 0.05$.

From figures 4(a)–(c), it can be seen that, although the drive network (18) is not internally synchronous because of the small coupling strength $\theta = 0.05$, the state variables of the

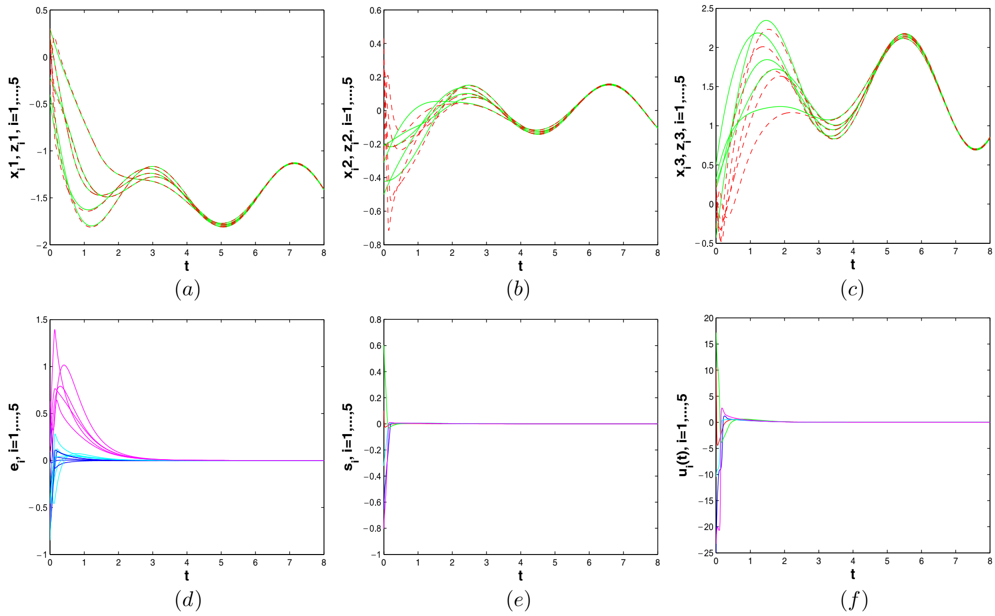

Figure 3. Synchronization of the drive–response network with the star-shaped coupling configuration and coupling strength $\theta = 1.5$. (*a*)–(*c*) Evolution of state variables x_i and z_i, (*d*) synchronization error states e_i, (*e*) time responses of s_i and (*f*) time responses of control inputs.

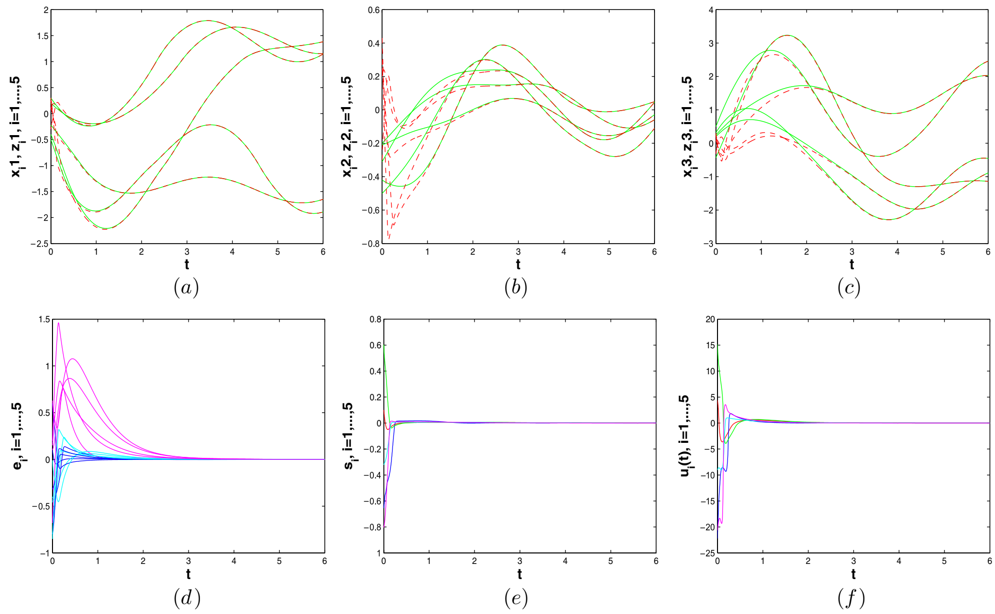

Figure 4. Synchronization of the drive–response network with the global coupling configuration and coupling strength $\theta = 0.05$. (*a*)–(*c*) Evolution of state variables x_i and z_i, (*d*) synchronization error states e_i, (*e*) time responses of s_i and (*f*) time responses of control inputs.

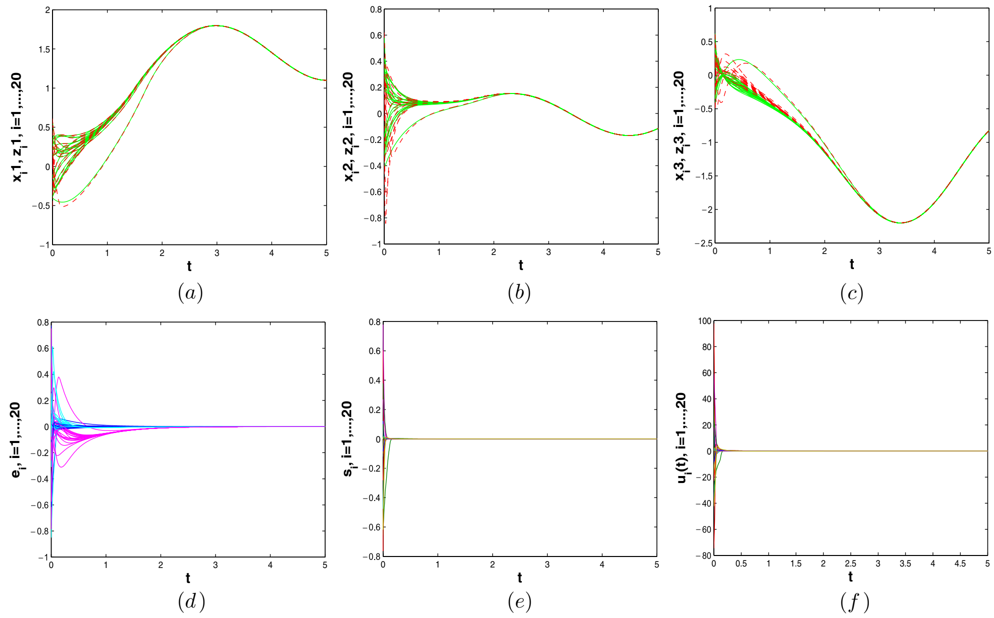

Figure 5. Synchronization of the drive–response network with the non-regularly coupling configuration and coupling strength $\theta = 4.5$. (*a*)–(*c*) Evolution of state variables x_i and z_i, (*d*) synchronization error states e_i, (*e*) time responses of s_i and (*f*) time responses of control inputs.

response network (19) still tend to those of the drive network. Figure 4(*d*) displaces the evolutions of the error variables $e_i(t)$, showing $e_i(t) \rightarrow 0$, as $t \rightarrow \infty$.

To further verify the theorems given in section 3, consider non-regularly coupled networks consisting of 20 nodes, generated by following the procedure of the well-known BA model. Figure 5 shows the synchronization of the drive–response network.

Figure 5 shows the effectiveness of the designed controller (8) for some cases where the node number of the drive–response network increases. Note that the controller is robust to the nonlinear inputs, the only constraint on which is given by (3). Furthermore, the chattering effect has been eliminated as a result of the continuity of the controller (8).

5. Conclusions

In this paper, a novel decentralized control scheme for global exponential synchronization of drive–response complex networks is derived. The feedback controller uses only individual node's information, without the need of communications among different nodes over the network. Further, due to the merit of the employed proportional–integral sliding mode control method, the control strategy is robust to input nonlinearity under certain conditions. The effectiveness and feasibility of the control strategy is confirmed and demonstrated by numerical simulations on chaotic drive–response networks with various coupling configurations. The approach developed in this paper may be further applied to complex networks synchronization subject to random inputs in the future. And research for the cases when the node numbers or coupling configurations of the drive and response networks are different seems promising and deserves further efforts.

Acknowledgments

This work is supported by the City University of Hong Kong under the Research Enhancement Scheme and SRG grant 7002134 and the National Science Foundation of China under grants 60674093.

References

[1] Boccaletti S, Latora V, Moreno Y, Chavezf M and Hwanga D U 2006 Complex networks: structure and dynamics *Phys. Rep.* **424** 175–308
[2] Fan J, Li X and Wang X F 2005 On synchronous preference of complex dynamical networks *Physica* A **335** 657–66
[3] Fan J, Li X and Wang X F 2005 On synchronization in scale-free dynamical networks *Physica* A **349** 443–51
[4] Li X and Chen G 2003 Synchronization and desynchronization of complex dynamical networks: an engineering viewpoint *IEEE Trans. Circuits Syst. I* **50** 1381–90
[5] Lü J H and Chen G 2004 Chaos synchronization of general complex dynamical networks *Physica* A **334** 281–302
[6] Motter A E, Zhou C S and Kurths J 2005 Enhancing complex network synchronization *Europhys. Lett.* **69** 334–40
[7] Barahona M and Pecora L M 2002 Synchronization in small-world systems *Phys. Rev. Lett.* **89** 1–4
[8] Hu G, Yang J Z and Liu W J 1998 Instability and controllability of linearly coupled oscillators: eigenvalues analysis *Phys. Rev.* E **58** 4440–53
[9] Kocarev L and Amato P 2005 Synchronization in power-law networks *Chaos* **15** 024101
[10] Lü J H, Yu X H, Chen G and Cheng D Z 2004 Characterizing the synchronizability of small-world dynamical networks *IEEE. Trans. Circuits Syst. I* **51** 787–96
[11] Pecora L M and Carroll T L 1998 Master stability functions for synchronized coupled systems *Phys. Rev. Lett.* **80** 2109–12
[12] Pecora L M, Carroll T, Johnson G, Mar D and Fink K S 2000 Synchronization stability in coupled oscillator arrays: solution for arbitrary configuration *Int. J. Bifurcation Chaos* **10** 273–90
[13] Wang X F and Chen G 2002 Synchronization in scale-free dynamical networks: robustness and fragility *IEEE Trans. Circuits Syst. I* **49** 54–62
[14] Nishikawa T, Motter A E, Lai Y C and Hoppensteadt F C 2003 Heterogeneity in oscillator networks: are smaller world easier to synchronize? *Phys. Rev. Lett.* **91** 1–4
[15] Wu C W 2001 Synchronization in arrays of coupled nonlinear systems: passivity, circle criterion and observer design *IEEE Trans. Circuits Syst. I* **48** 1257–61
[16] Xiang L Y, Chen Z Q, Liu Z X, Chen F and Yuan Z Z 2007 Stabilizing weighted complex networks *J. Phys. A: Math. Theor.* **40** 14369–82
[17] Chen T P, Liu X W and Lu W L 2007 Pinning complex networks by a single controller *IEEE Trans. Circuits Syst. I* **54** 1317–26
[18] Fan Z P and Chen G 2005 Pinning control of scale-free complex networks *Proc. IEEE Int. Symp. on Circuits and Systems* vol 1 pp 284–7
[19] Li X, Wang X and Chen G 2004 Pinning a complex dynamical network to its equilibrium *IEEE Trans. Circuits Syst. I* **51** 2074–87
[20] Sorrentino F, di Bernardo M, Garofalo F and Chen G 2007 Controllability of complex networks via pinning *Phys. Rev.* E **75** 046103
[21] Wang X F and Chen G 2002 Pinning control of scale-free dynamical networks *Physica* A **310** 521–31
[22] Li C P, Sun W G and Kurths J 2007 Synchronization between two coupled complex networks *Phys. Rev.* E **76** 046204
[23] Duan Z S, Wang J Z and Huang L 2007 Special decentralized control problems in discrete-time interconnected systems composed of two subsystems *Syst. Control Lett.* **56** 206–14
[24] Huang S D and Zhang S Y 1998 Comments on 'Design of decentralized control for symmetrically interconnected systems' *Automatica* **34** 929–33
[25] Siljak D D 1991 *Decentralized Control of Complex Systems* (New York: Academic)
[26] Hsu K C 1998 Variable structure control design for uncertain dynamic systems with sector nonlinearities *Automatica* **34** 505–8
[27] Pecora L M and Carroll T L 1991 Driving systems with chaotic signals *Phys. Rev.* A **44** 2374–83
[28] Agiza H N and Yassen M T 2001 Synchronization of Rössler and Chen chaotic dynamical systems using active control *Phys. Lett.* A **278** 191–7

[29] Etemadi S, Alasty A and Salarieh H 2006 Synchronization of chaotic systems with parameter uncertainties via variable structure control *Phys. Lett.* A **357** 17–21

[30] Ho M C and Hung Y C 2002 Synchronization of two different systems by using generalized active control *Phys. Lett.* A **301** 424–8

[31] Tavazoei M S and Haeri M 2007 Determination of active sliding mode controller parameters in synchronizing different chaotic systems *Chaos Solitons Fractals* **32** 583–91

[32] Lin J S, Yan J J and Liao T L 2005 Chaotic synchronization via adaptive sliding mode observers subject to input nonlinearity *Chaos Solitons Fractals* **24** 371–81

[33] Utkin V I 1978 *Sliding Mode and their Applications in Variable Structure Systems* (Moscow: Mir)

[34] Chua L O 2002 A zoo of strange attractors from the canonical Chua's circuits *Proc. 35th Midwest Symp. Circuit and Systems* vol 2 pp 916–26